Article

Cell PRESS

Nitrate-Regulated Auxin Transport by NRT1.1 Defines a Mechanism for Nutrient Sensing in Plants

Gabriel Krouk,[1,5] Benoît Lacombe,[1] Agnieszka Bielach,[2] Francine Perrine-Walker,[1] Katerina Malinska,[3] Emmanuelle Mounier,[1] Klara Hoyerova,[3] Pascal Tillard,[1] Sarah Leon,[1] Karin Ljung,[4] Eva Zazimalova,[3] Eva Benkova,[2] Philippe Nacry,[1] and Alain Gojon[1,*]

[1]Biochimie et Physiologie Moléculaire des Plantes, UMR 5004 CNRS/INRA/SupAgro-M/UM2, Institut de Biologie Intégrative des Plantes, Place Viala, 34060 Montpellier Cedex 1, France
[2]Flanders Institute for Biotechnology, Department of Plant Systems Biology, Ghent University, Technologiepark 927, 9052 Gent, Belgium
[3]Institute of Experimental Botany, Academy of Sciences of the Czech Republic, Rozvojová 263, 16502 Prague 6, Czech Republic
[4]Umea Plant Science Center, Department of Forest Genetics and Plant Physiology, Swedish University of Agricultural Sciences, SE-901 83 Umea, Sweden
[5]Present address: Department of Biology, New York University, 100 Washington Square East, New York, NY 10003, USA
*Correspondence: gojon@supagro.inra.fr

SUMMARY

Nitrate is both a nitrogen source for higher plants and a signal molecule regulating their development. In *Arabidopsis*, the NRT1.1 nitrate transporter is crucial for nitrate signaling governing root growth, and has been proposed to act as a nitrate sensor. However, the sensing mechanism is unknown. Herein we show that NRT1.1 not only transports nitrate but also facilitates uptake of the phytohormone auxin. Moreover, nitrate inhibits NRT1.1-dependent auxin uptake, suggesting that transduction of nitrate signal by NRT1.1 is associated with a modification of auxin transport. Among other effects, auxin stimulates lateral root development. Mutation of *NRT1.1* enhances both auxin accumulation in lateral roots and growth of these roots at low, but not high, nitrate concentration. Thus, we propose that NRT1.1 represses lateral root growth at low nitrate availability by promoting basipetal auxin transport out of these roots. This defines a mechanism connecting nutrient and hormone signaling during organ development.

INTRODUCTION

The mineral nutrition of most terrestrial organisms (bacteria, fungi, plants) relies on the uptake of inorganic ions from the soil. However, the availability of these ions dramatically fluctuates in both time and space, which makes nutrient-limiting conditions a general rule in natural ecosystems. To face this constraint, all organisms develop adaptive responses triggered by sensing systems that perceive external nutrient availability (Gojon et al., 2009; Hoch, 2000; Holsbeeks et al., 2004; Schachtman and Shin, 2007). Sensors of external nutrients have mostly been identified in bacteria, where they predominantly belong to the general class of two-component and phosphorelay signal

transduction systems (Hoch, 2000). In eukaryotes, knowledge is mostly limited to the yeast *Saccharomyces cerevisiae*, where mineral nutrient sensing is apparently ensured by other systems, for example, transceptor proteins located at the plasma membrane which fulfill a dual transport/sensing function (Holsbeeks et al., 2004). However, there is so far no clue on how these proteins transform the external nutrient concentration into a signal transduced into the cell.

To date, mineral nutrient sensors are mostly uncharacterized in plants (Schachtman and Shin, 2007), but recent findings in *Arabidopsis thaliana* suggest that the plasma membrane nitrate (NO_3^-) transporter NRT1.1 (CHL1), initially characterized as an influx carrier participating in the root uptake of NO_3^- from the soil solution (Tsay et al., 1993), also plays a role in NO_3^- signaling, and acts as an NO_3^- sensor (Ho et al., 2009; Krouk et al., 2006, 2010; Muños et al., 2004; Remans et al., 2006; Walch-Liu and Forde, 2008; Wang et al., 2009). Nitrate is not only the main nitrogen source for many higher plants but also a major signal molecule modulating plant metabolism and growth (Crawford, 1995; Stitt, 1999). The signaling effect of NO_3^- is particularly strong on the development of lateral roots (LRs), which emerge postembryonically and determine the branching pattern of the root system (Forde, 2002; Malamy, 2005). NRT1.1 is crucial for the NO_3^- regulation of root system architecture, because it triggers a specific NO_3^--signaling pathway that stimulates LR growth in response to a localized supply of NO_3^- (Remans et al., 2006). As such, NRT1.1 plays an important role in the adaptive response of the plant to nitrogen limitation because it directs preferential growth of LRs in NO_3^--rich patches of the external medium.

Our aim was to investigate the mechanisms involved in the NRT1.1-dependent signaling pathway responsible for stimulation of LR growth by NO_3^-. Three considerations prompted us to examine the putative connection between NRT1.1 and the phytohormone auxin: (1) auxin plays a central role in plant development (Benjamins and Scheres, 2008; Teale et al., 2006; Vanneste and Friml, 2009), and is particularly responsible for stimulation of both initiation and growth of LRs (Benkova et al., 2003; Casimiro et al., 2003; De Smet et al., 2007; Laskowski et al., 2008); (2) the NO_3^--signaling pathway responsible for

stimulation of LR growth was proposed to involve auxin at an unknown step of signal transduction (Forde, 2002; Zhang et al., 1999); and (3) *NRT1.1* expression is strongly induced by auxin (Guo et al., 2002). These data suggest that auxin may be a secondary signal or a trigger mediating the regulatory action of NRT1.1 on LR development.

Therefore, to study the role of auxin in the NRT1.1-dependent NO_3^--signaling pathway, we examined how NRT1.1 affects auxin accumulation/sensitivity in *Arabidopsis* LRs. The present work demonstrates that NRT1.1 regulates root branching because it exerts an NO_3^--dependent control on auxin accumulation in LRs. This is due to the unexpected functional property of this protein which, in addition to transporting NO_3^-, facilitates auxin transport and its fine-tuning by NO_3^-. A model is proposed to explain how NO_3^--regulated auxin transport, dependent on NRT1.1, accounts for the effects of external NO_3^- availability on auxin gradients in LRs and growth of these LRs in *Arabidopsis* seedlings.

RESULTS

NRT1.1 Represses Auxin Accumulation in LR Primordia and Young LRs at Low External NO_3^- Concentration

To investigate the role of NRT1.1 in auxin signaling in roots of *Arabidopsis* seedlings, we used a line expressing the auxin-inducible *DR5::GUS* reporter gene (Ulmasov et al., 1997) that we crossed with the *chl1-5* knockout mutant for *NRT1.1*. In wild-type background, the supply of 1 mM NO_3^- as compared to N-free medium resulted in a strong increase in *DR5::GUS* expression in LR primordia prior to emergence and in young LRs, but not in newly initiated primordia (Figure 1A). This response appears to be quantitative (0.2 mM NO_3^- had a lower impact), and specific of NO_3^- because supply of an alternative N source (0.5 mM glutamine) had no effect. Mutation of *NRT1.1* did not affect expression of *DR5::GUS* in plants supplied with 1 mM NO_3^-, but dramatically increased it in plants either grown in the absence of NO_3^- (N-free medium or 0.5 mM glutamine) or supplied with a low external NO_3^- concentration (0.2 mM). Thus, the absence of a functional NRT1.1 transporter prevented the decrease of *DR5::GUS* expression in response to removal or lowered supply of NO_3^-, leading to a high *DR5* activity regardless of the presence of an N source. The *DR5::GUS* reporter was still responsive to indole-3-acetic acid (IAA) or naphthalene-1-acetic acid (NAA) supply in *chl1-5xDR5::GUS* plants (see Figure S1A available online), indicating that its overexpression in *chl1-5* roots does not result from a deregulated auxin-signaling pathway but more likely reflects an increase in local auxin concentrations. This was confirmed by IAA immunolocalization in LR tips (Figure 1B). However, total IAA accumulation in the whole root system was similar in wild-type and *chl1-5* plants (Figure S1B), suggesting that *NRT1.1* mutation might lead to very localized changes in auxin concentration in emerging LRs. Altogether, the above data show that NRT1.1 is required to prevent auxin accumulation in preemerged LR primordia and young LRs when external NO_3^- concentration is null or at a low level. In contrast, auxin accumulation in initiating primordia appeared to be independent of both NO_3^- and NRT1.1.
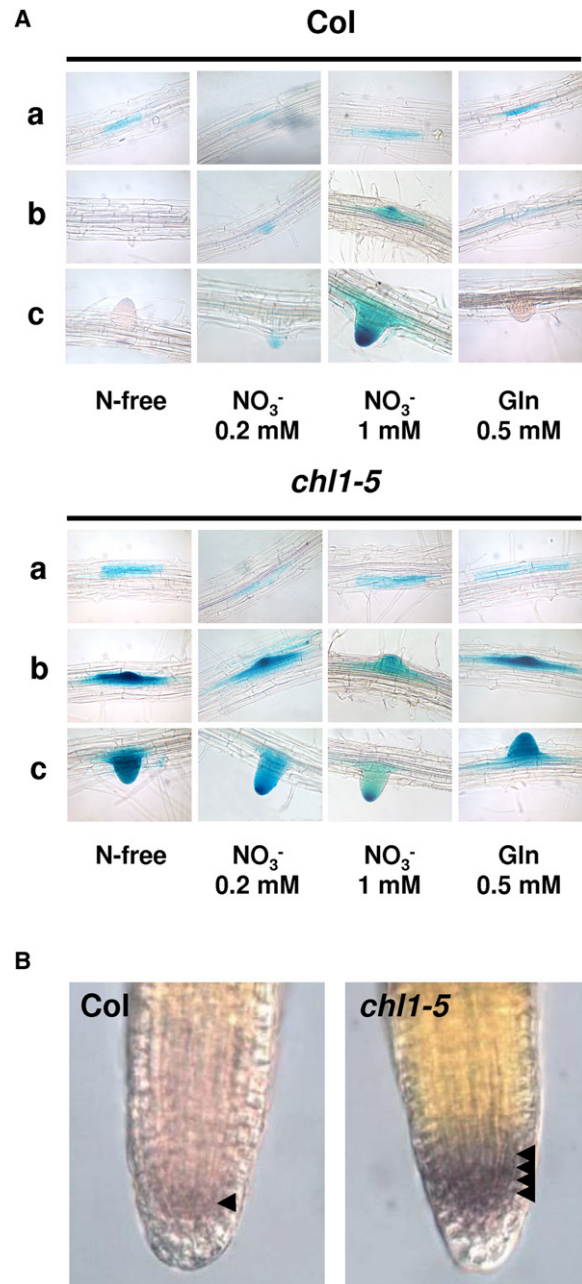

Figure 1. Nitrate Dependence of Increased Auxin Accumulation in Lateral Root Primordia and Young Lateral Roots Resulting from *NRT1.1* Mutation

(A) Histochemical staining of GUS activity in lateral root primordia and newly emerged lateral roots of transgenic *Arabidopsis* plants expressing *DR5::GUS* in wild-type or *chl1-5* background. Three stages of development are considered: initiating primordia (a), primordia prior to emergence (b), and newly emerged lateral roots (c). The plants were cultivated for 8 days on media containing nitrogen sources described in the figure.

(B) IAA immunolocalization in LR tips of wild-type and *chl1-5* plants. The IAA signal (dark area) in the LR tip is indicated by the arrowheads. The pictures shown are representative of 13 and 34 independent replicates for Col and *chl1-5* seedlings, respectively. See also Figure S1.
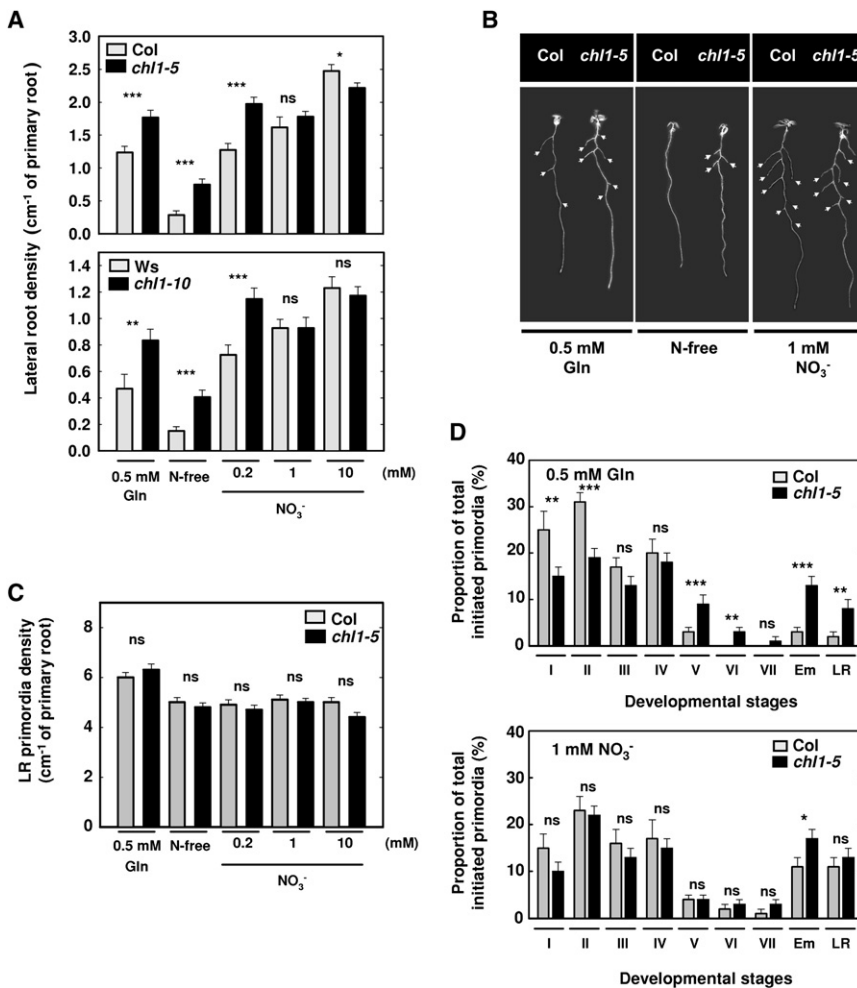
Figure 2. chl1 Mutation Promotes Lateral Root Growth in the Absence or at Low Concentration of NO_3^-

(A) Density of visible (>0.5 mm) lateral roots in plants (Col, chl1-5, Ws, chl1-10) grown for 8 days on media containing nitrogen sources described in the figure. Results (n = 30–52) are representative of three independent experiments. Differences between mutant and wild-type genotypes are statistically significant at *$p < 0.05$; **$p < 0.01$; ***$p < 0.001$ (t test). ns, not significant.

(B) Selected pictures figuring chl1-5 root phenotype. Arrowheads indicate visible lateral roots.

(C) Density of lateral root primordia initiated on the primary root of Col and chl1-5 plants grown for 8 days on media containing nitrogen sources described in the figure (n = 20).

(D) Distribution of lateral root primordia between various stages of development (Em, emerged primordia; LR, lateral root) in Col and chl1-5 plants grown either on 0.5 mM glutamine or 1 mM NO_3^- as an N source. Results (n = 20) are expressed as the proportion of total lateral root primordia initiated.

Differences between mutant and wild-type genotypes are statistically significant at *$p < 0.05$; **$p < 0.01$; ***$p < 0.001$ (t test). ns, not significant. See also Figure S2.

affinity NO_3^- transporter also involved in root NO_3^- uptake (Huang et al., 1999) but which, unlike NRT1.1, does not seem to have a signaling role (Krouk et al., 2006). In contrast to chl1 mutants, atnrt1.2-1 plants showed little alteration, if any, of LR density as compared to the wild-type, regardless of the N treatment (Figure S2A). This demonstrates that NRT1.1, but not NRT1.2, regulates root branching in response to NO_3^-.

We then performed microscopic analyses to determine frequency of lateral root initiation and distribution of developmental stages (Malamy and Benfey, 1997) in chl1-5 and wild-type roots. Under our conditions, neither NO_3^- concentration nor NRT1.1 mutation affected the density of primordia initiated on the primary root (Figure 2C). However, both NO_3^- and NRT1.1 had impact on primordia development and modified their distribution between the various developmental stages (Figure 2D). Supplying 1 mM NO_3^- instead of 0.5 mM glutamine to wild-type plants increased the proportion of primordia that progressed in development to late stages (Em and LR). The mutation of NRT1.1 mimics this high-NO_3^- effect on LR development. Indeed, in glutamine-fed plants, the proportion of emerged primordia or LRs was much higher in chl1-5 than in wild-type (Figure 2D). This indicates that NRT1.1 does not regulate initiation of LR primordia, but slows down their development in the absence of NO_3^-.

Our data show that in the absence or at low availability of NO_3^-, NRT1.1 represses accumulation of auxin (Figure 1) and inhibits growth of preemerged LR primordia and young LRs (Figure 2). We thus hypothesized that NRT1.1 modulates LR

NRT1.1 Represses LR Growth at Low External NO_3^- Concentration

To relate these data to our previous results showing that NRT1.1 is required for directing preferential LR growth in NO_3^--rich patches of the external medium (Remans et al., 2006), we investigated how NRT1.1 mutation alters root branching of seedlings as a function of the external NO_3^- concentration. Therefore, we measured the density of visible LRs (>0.5 mm) on chl1-5 and chl1-10 knockout mutants and their control wild-types. Growth of the primary root was almost independent of NO_3^- supply and of NRT1.1 (data not shown). However, the increase in external NO_3^- concentration from 0 to 10 mM led to a marked increase in the density of visible LRs in both Col and Ws plants (Figures 2A and 2B). When compared to wild-types, both chl1-5 and chl1-10 plants displayed a higher density of visible LRs in the absence or at low (0.2 mM) concentration of NO_3^-, whereas at high NO_3^- concentration (1 or 10 mM), LR density of mutants did not significantly differ from that of control seedlings (Figures 2A and 2B). As for DR5::GUS activity, the increased LR density phenotype of chl1 mutants is not suppressed by supply of 0.5 mM glutamine. To clarify the specific role of NRT1.1 in the NO_3^- regulation of LR growth, we used the atnrt1.2-1 knockout mutant as a control. NRT1.2 is a low-
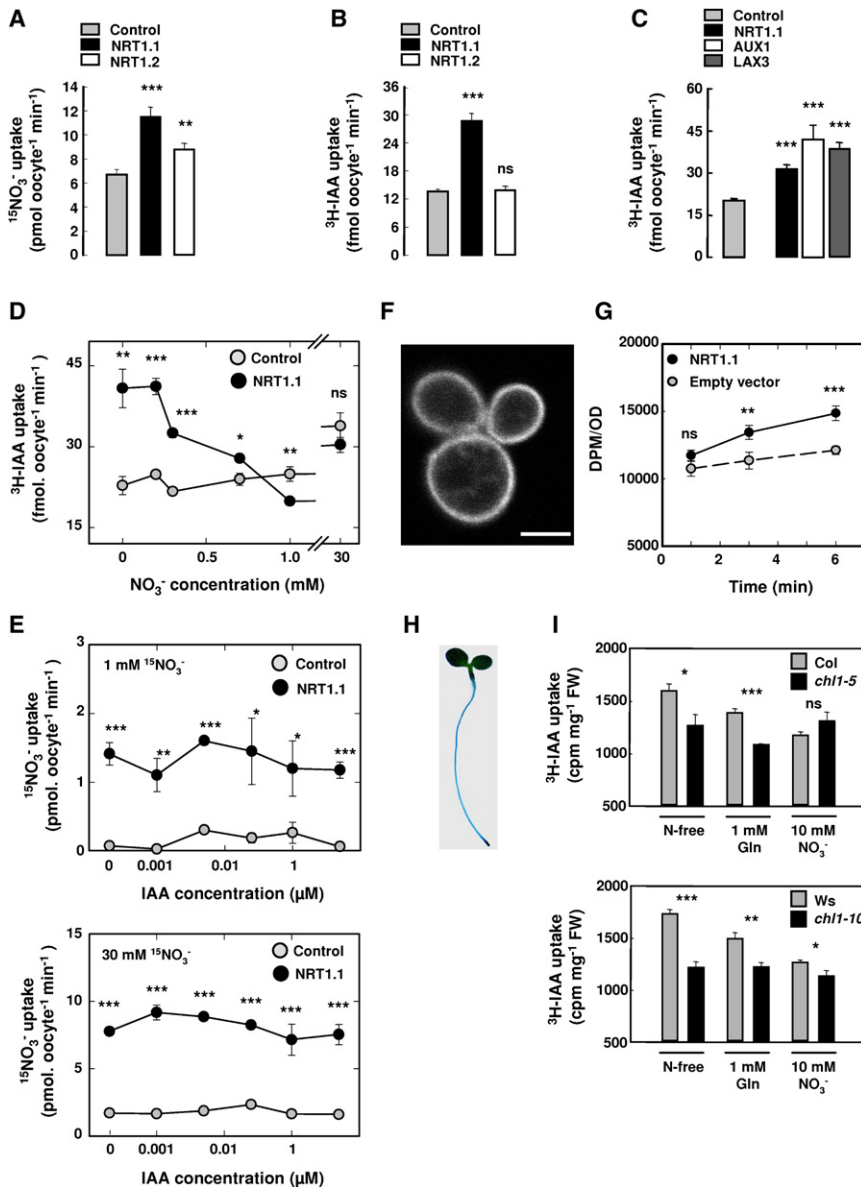
Figure 3. NRT1.1 Facilitates NO$_3^-$-Inhibited Auxin Influx in Heterologous Expression Systems and In Planta

(A) ^{15}NO$_3^-$ uptake in NRT1.1-cRNA- or NRT1.2-cRNA-injected and control *Xenopus* oocytes supplied with 30 mM ^{15}NO$_3^-$. Results (n = 6 batches of five oocytes) are representative of five and three independent experiments for NRT1.1 and NRT1.2, respectively (each experiment was performed with oocytes from a different frog). Data were analyzed through one-way ANOVA, three-level factor (control; NRT1.1; NRT1.2), p = 9.0 e-06, followed by a t test as a post hoc analysis.

(B) [^{3}H]IAA uptake in NRT1.1-cRNA- or NRT1.2-cRNA-injected and control *Xenopus* oocytes supplied with 1 μM [^{3}H]IAA. Results (n = 24–30) are representative of five and three independent experiments for NRT1.1 and NRT1.2, respectively (each experiment was performed with oocytes from a different frog). Data were analyzed through one-way ANOVA, three-level factor (control; NRT1.1; NRT1.2), p = 2.2 e-16, followed by a t test as a post hoc analysis.

(C) [^{3}H]IAA uptake in NRT1.1-cRNA-, AUX1-cRNA-, and LAX3-cRNA-injected and control *Xenopus* oocytes supplied with 1 μM [^{3}H]IAA (n = 7–18).

(D) Effect of increasing NO$_3^-$ concentration on [^{3}H]IAA uptake in NRT1.1-cRNA-injected and control *Xenopus* oocytes supplied with 1 μM [^{3}H]IAA (n = 8–22).

(E) Effect of increasing IAA concentration on ^{15}NO$_3^-$ uptake in NRT1.1-cRNA-injected and control *Xenopus* oocytes supplied with either 1 or 30 mM ^{15}NO$_3^-$ (n = 4–8).

(F) Fluorescence micrograph of *S. cerevisiae* strain BY4742 expressing NRT1.1-GFP. The scale bar represents 5 μm.

(G) [^{3}H]IAA uptake in yeast strain BY4742 expressing NRT1.1 and a control strain transformed with empty vector. Results (n = 11) are means of data obtained in three independent experiments with three or four replicates each. DPM, disintegrations per minute; OD, optical density.

(H) Histochemical staining of GUS activity in 4-day-old transgenic *Arabidopsis* seedlings expressing *pNRT1.1::GUS*.

(I) [^{3}H]IAA uptake in seedlings (Col, *chl1-5*, Ws, *chl1-10*) grown for 4 days on media containing nitrogen sources described in the figure. Results (n = 5 batches of ten seedlings) are representative of three independent experiments. Differences are statistically significant at *p < 0.05; **p < 0.01; ***p < 0.001 (t test). ns, not significant. See also Figure S3.

growth by controlling auxin accumulation in these organs. Accordingly, exogenous supply of IAA phenocopied *NRT1.1* mutation, because retarded LR development in wild-type plants grown on 0.5 mM glutamine was recovered by exogenous auxin (Figure S2B). This is consistent with the proposal that on NO$_3^-$-free medium, slower LR growth in wild-type plants than in *chl1* mutants is due to suboptimal auxin levels in LRs.

NRT1.1 Displays an Auxin Transport Facilitation Inhibited by High NO$_3^-$ Concentration

The observation that NRT1.1 represses local auxin accumulation in LR tips of plants grown on an NO$_3^-$-free medium raises the question of how an NO$_3^-$ transporter might affect hormone localization when NO$_3^-$ is not present. Altered root growth in *chl1*

mutants on NO$_3^-$-free media has already been reported (Guo et al., 2001), but to date no hypothesis has been proposed to account for these unexpected findings. One possibility is that NRT1.1 may transport substrates other than NO$_3^-$, as suggested by the demonstration that its *Brassica napus* homolog (BnNRT1.2) mediates not only NO$_3^-$ but also amino acid transport (Zhou et al., 1998). We therefore investigated whether auxin can be a substrate for NRT1.1, using *Xenopus* oocytes as a heterologous expression system and NRT1.2 as a control. We first verified that oocytes injected with NRT1.1 or NRT1.2 cRNA displayed an increase in ^{15}NO$_3^-$ influx into the cell, as compared with control oocytes (Figure 3A). We then investigated IAA transport by supplying [^{3}H]IAA at 1 μM in the assay medium without NO$_3^-$. As noticed in previous studies on AUX1

(Yang et al., 2006) and LAX3 (Swarup et al., 2008), a basal level of [^{3}H]IAA accumulation was recorded in control oocytes (Figure 3B). Injection of NRT1.1 cRNA resulted in a significant increase of [^{3}H]IAA uptake in oocytes, whereas NRT1.2 cRNA had no effect (Figure 3B). This shows that NRT1.1, but not NRT1.2, is able to transport auxin or to facilitate auxin transport in a heterologous system. [^{3}H]IAA uptake by NRT1.1 in oocytes was lower but still significant as compared with that mediated by AUX1 or LAX3 (Figure 3C). It was markedly reduced by an excess of unlabeled IAA (Figure S3A), but was not significantly affected by the auxin transport inhibitors TIBA, NPA, or 1-NOA (Figure S3B). Most interestingly, an increase in external NO$_3^-$ concentration in the range of 0–1 mM gradually suppressed [^{3}H]IAA overaccumulation in oocytes injected with NRT1.1 cRNA, without reducing [^{3}H]IAA uptake in control oocytes (Figure 3D). This shows that auxin transport facilitation by NRT1.1 is inhibited by NO$_3^-$. However, the reverse was not true, because auxin had no effect on ^{15}NO$_3^-$ uptake by NRT1.1 when assayed at either 1 or 30 mM external concentration (Figure 3E).

To confirm facilitation of auxin transport by NRT1.1, we used other established systems for measurement of auxin transport activity, such as yeast or BY-2 tobacco cells (Petrasek et al., 2006). NRT1.1 as well as NRT1.1 fused to GFP were expressed in *S. cerevisiae*. Figure 3F shows that NRT1.1-GFP was localized at the yeast plasma membrane. In yeast whole-cell IAA transport assays, a weak but highly statistically significant increase in [^{3}H]IAA accumulation was recorded in NRT1.1-expressing cells as compared to the empty vector control (Figure 3G). That only a small relative difference is found between NRT1.1-expressing cells and controls is a very common observation in functional studies of plant auxin influx carriers using a yeast expression system (Yang and Murphy, 2009). Evidence for increased auxin transport associated with NRT1.1 expression was also obtained in BY-2 cell-suspension cultures (Figure S3C). To further document an NO$_3^-$-dependent auxin influx activity associated with NRT1.1 in planta, we then assayed uptake of exogenous [^{3}H]IAA in wild-type and *chl1* mutants at a young stage (4-day-old plants), when *NRT1.1* is strongly expressed in most tissues, including the whole primary root that at this stage lacks visible laterals (Figure 3H). Therefore, we quantified total radioactivity accumulated in seedlings following short-term (30 min) transfer to a [^{3}H]IAA-labeled liquid basal medium of the same composition as that used for growth in vertical Petri dishes. The data showed that mutation of *NRT1.1* results in a significant decrease of [^{3}H]IAA uptake by the plant in the absence but not in the presence of NO$_3^-$ (Figure 3I). In agreement with the oocyte data, the *atnrt1.2-1* knockout mutant for *NRT1.2* did not show any reduction in exogenous [^{3}H]IAA uptake on N-free medium (Figure S3D). From these observations, we conclude that as in oocytes, yeast, and BY-2 cells, NRT1.1 can function as an auxin influx facilitator in *Arabidopsis* roots, contributing to an auxin transport activity modulated by NO$_3^-$.

Using *pNRT1.1::GUS* fusions, *NRT1.1* expression has been shown to be strong in LR primordia and LR tips (Guo et al., 2001; Remans et al., 2006). An intriguing aspect of our results is that, although we detect auxin influx facilitation by NRT1.1 (Figure 3), its absence in the *chl1-5* mutant leads to higher auxin accumulation in LR primordia and LR tips (Figure 1) at low NO$_3^-$

concentration. This indicates that NRT1.1 acts in preventing, and not promoting, auxin accumulation in the tissues where it is expressed.

Membrane Localization of NRT1.1 Suggests a Role in the Basipetal Transport of Auxin Out of LR Tips

Auxin gradient in LR primordia and root tips is generated by the activity of various auxin transporters, including AUX/LAX influx transporters and PIN and ABCB (formerly MDR/PGP) efflux carriers (Benjamins and Scheres, 2008; Benkova et al., 2003; Blilou et al., 2005; Kramer and Bennett, 2006; Swarup et al., 2008; Vanneste and Friml, 2009; Vieten et al., 2007; Wu et al., 2007). According to the so-called fountain model for LRs, auxin moves from the root vasculature acropetally via the interior of the LR into the tip, from which it is transported away by a basipetal transport route through the outer cell layer (Benkova et al., 2003). To understand how NRT1.1 may alter auxin transport and accumulation in LRs, we determined the pattern of both *NRT1.1* gene expression and NRT1.1 protein localization.
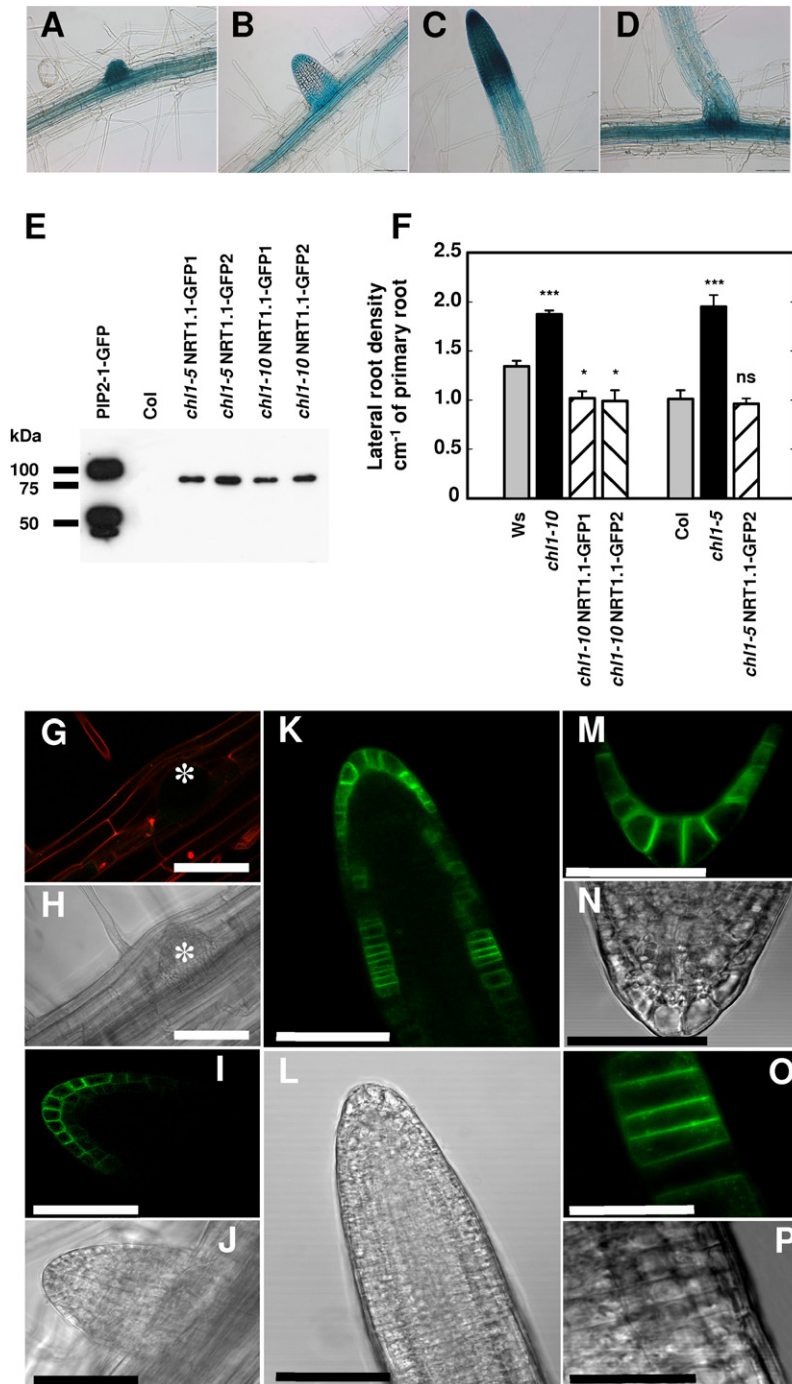
As described previously (Guo et al., 2001; Remans et al., 2006), histochemical GUS staining in *pNRT1.1::GUS* transgenic plants showed that *pNRT1.1* is mostly active in the stele, in LR primordia before emergence, and in the tip and basis of emerged LR primordia and young LRs (Figures 4A–4D). We then generated *pNRT1.1::NRT1.1-GFP* transformants in both *chl1-5* and *chl1-10* backgrounds. The presence of the NRT1.1-GFP protein in the membrane fractions isolated from seedlings of four independent lines was verified by western blotting (Figure 4E). Three of these lines displayed a full complementation of the *chl1* mutant phenotype for LR density (Figure 4F), and were used for NRT1.1-GFP localization studies in LRs (Figures 4G–4P). Unexpectedly, no NRT1.1-GFP signal was recorded in LR primordia at young stages (Figures 4G and 4H). However, it begins to appear in the outermost cell layer of the LR tip just before emergence (Figures 4I and 4J). In elongating young LRs not yet visible (<0.5 mm), NRT1.1-GFP is localized in the outermost layer of cells, all along from the tip to the base of the LR (Figures 4K and 4L). In these cells, the GFP signal appears to be very low in the periclinal sides facing the external medium, but much stronger in the anticlinal faces separating these cells (Figures 4M–4P). This localization pattern was confirmed by NRT1.1-GFP immunolocalization (Figure S4). Neither the localization pattern of *pNRT1.1* activity nor that of the NRT1.1-GFP protein was modified by the N source supplied to the plants (0.5 mM glutamine or 1 mM NO$_3^-$; data not shown).

Altogether, these data allow a hypothesis to be proposed for the putative role of NRT1.1 in preventing auxin accumulation in LRs. Indeed, in emerging primordia and young LRs, NRT1.1-GFP localization matches that of the basipetal transport route for auxin (Benkova et al., 2003), suggesting that NRT1.1 may be involved in taking up auxin into the epidermal cells, thus injecting the hormone into its reflux pathway from the tip to the base of the LRs.

DISCUSSION

NRT1.1-Dependent Auxin Transport
Although unexpected at first glance, auxin influx facilitation by NRT1.1 makes an interesting parallel with the AUX/LAX auxin

Figure 4. Localization of *pNRT1.1* Activity and NRT1.1-GFP Protein in Root Tissues

(A–D) Histochemical localization of GUS activity in primary root and lateral root primordia (A and B) and young lateral roots (C and D) of *pNRT1.1::GUS* plants.

(E) Western blot with anti-GFP antibody on microsomal fractions isolated from *pPIP2.1::PIP2.1-GFP* plants, Col plants, and four independent *pNRT1.1::NRT1.1-GFP* lines. *pPIP2.1::PIP2.1-GFP* and Col plants were used as positive and negative controls for the specificity of the anti-GFP antibody, respectively.

(F) Complementation of the lateral root development phenotype of *chl1* mutant by the *pNRT1.1::NRT1.1-GFP* construct. Plants were grown on 0.5 mM glutamine as an N source, and experiments were performed as described in Figure 2A (n = 12–19). Differences are statistically significant at *p < 0.05; ***p < 0.001 (t test). ns, not significant.

(G–P) NRT1.1-GFP localization in root tissues of *pNRT1.1::NRT1.1-GFP* plants.

(G) NRT1.1-GFP in an unemerged lateral root primordium (propidium iodide staining in red). The asterisks visualize the location of the primordium.

(H) Differential interference contrast (DIC) image corresponding to (G).

(I) NRT1.1-GFP in emerging primordium.

(J) DIC image corresponding to (I).

(K, M, and O) NRT1.1-GFP in young lateral root.

(L, N, and P) DIC images corresponding to (K), (M), and (O). The plants were grown for 9 days on glutamine as nitrogen source.

The scale bars represent 50 μm, except 25 μm for (O) and (P). The pictures shown are representative of >50 primordia and >30 lateral roots from >20 plants of three independent lines. See also Figure S4.

esis that the changes observed for auxin accumulation in LRs directly result from auxin transport by NRT1.1. First, expression of NRT1.1 in oocytes, yeast, or tobacco cells stimulates auxin uptake by the cell. The fact that expression of NRT1.2 did not have the same effect (Figure 3B) argues against the possibility that this stimulation is an artifact resulting from heterologous expression of an anion carrier. Second, impaired auxin uptake was found in *chl1* mutants, but not in the *atnrt1.2-1* mutant, showing a specific role for NRT1.1 in auxin transport in planta (Figure 3I; Figure S3D). Third, the increase in auxin accumulation in LRs resulting from *NRT1.1* mutation cannot be accounted for by indirect effects, such as

influx carriers previously identified in plants (Kramer and Bennett, 2006; Swarup et al., 2008; Yang et al., 2006). Indeed, NRT1.1 and AUX/LAX proteins are classified within separate transporter families (PTR and ATF1, respectively) which share the common characteristic of including amino acid carriers (Williams and Miller, 2001; Wipf et al., 2002). Given the strong structural similarity between auxin and amino acids like tryptophan, it is not surprising to also find auxin transporters within these two families. Several lines of evidence support the hypoth-

changes in transmembrane potential or apoplastic pH, related to the fact that NRT1.1 is an H^+/NO_3^- symporter (Tsay et al., 1993). This is an important point to clarify, because such changes may alter auxin influx either by modifying the equilibrium between protonated/deprotonated forms of auxin in the apoplasm or by affecting the driving force for auxin uptake by other auxin carriers (Kramer and Bennett, 2006; Vanneste and Friml, 2009). If auxin overaccumulation in LRs of *chl1* plants is due to putative apoplastic pH or transmembrane potential

changes associated with the loss of H^+/NO_3^- symport by NRT1.1, it is predicted that this phenotype will be more pronounced at high NO_3^- (i.e., when H^+/NO_3^- symport by NRT1.1 is active). We can reject this hypothesis because we observed exactly the opposite. Indeed, the highest difference in *DR5::GUS* staining in LRs between wild-type and *chl1* plants was recorded in the absence of NO_3^-: the conditions where NRT1.1, by definition, cannot act as an H^+/NO_3^- symporter (Figure 1). However, because interaction between proteins displaying an auxin transport activity in heterologous systems (e.g., PIN and ABCB/PGP) has already been shown to occur (Blakeslee et al., 2007), we cannot presently rule out the hypothesis that the changes in auxin gradients seen in *chl1* mutants may result from an NO_3^--dependent effect of NRT1.1 on other auxin carriers.

The observation that NRT1.1-dependent auxin transport is inhibited by NO_3^- (Figures 3D and 3I) is at the center of the role of this protein in the NO_3^- regulation of LR growth. The mechanism of this inhibition is not known, but it does not seem to be due to simple substrate competition at the transport site because auxin does not affect NO_3^- transport by NRT1.1 (Figure 3E). Very recently, it has been demonstrated that the sensing function of NRT1.1 may be separate from its NO_3^- transport activity because specific point mutations of NRT1.1 (e.g., T101A, T101D, P492L) affect only one of these processes (Ho et al., 2009; Walch-Liu and Forde, 2008). Accordingly, Ho et al. (2009) proposed that NRT1.1-dependent sensing is activated by conformational changes of the NRT1.1 protein triggered by NO_3^- binding to specific recognition sites not involved in the transport function. Our data support this model because NO_3^- binding to such recognition sites can explain why NRT1.1-dependent auxin transport is inhibited by NO_3^-, and not vice versa. NRT1.1 has been proposed to act as a dual-affinity NO_3^- transporter and dual-affinity NO_3^- sensor, depending on the phosphorylation of the T101 residue. Phosphorylated NRT1.1 is a high-affinity NO_3^- transporter (Liu and Tsay, 2003) and triggers only high-affinity NO_3^- sensing (Ho et al., 2009), whereas nonphosphorylated NRT1.1 is a low-affinity NO_3^- transporter (Liu and Tsay, 2003) but is, however, able to trigger both high- and low-affinity NO_3^- sensing (Ho et al., 2009). It is not possible from the present study to determine a specific role of the phosphorylated or nonphosphorylated forms of NRT1.1 in auxin transport and signaling governing lateral root growth. Indeed, the observation that NO_3^- inhibition of NRT1.1-dependent auxin transport occurs in the low concentration range (0–0.5 mM NO_3^-; see Figure 3D) may suggest a specific involvement of the high-affinity NO_3^--sensing activity of NRT1.1, but because both forms of NRT1.1 activate this signaling, we cannot make conclusions on the specific involvement of one of these forms. Furthermore, our data of $^{15}NO_3^-$ uptake in NRT1.1-expressing oocytes at 1 mM (high-affinity) or 30 mM (low-affinity) external concentration (Figure 3E) indicate that both phosphorylated and nonphosphorylated forms of NRT1.1 are likely to be present in these oocytes, precluding any hypothesis on which one of these forms may be responsible for auxin transport. Only an extensive investigation of various T101 mutants of *NRT1.1*, both in heterologous expression systems and in planta, will allow conclusions on these aspects.

Localized Expression of the NRT1.1 Protein Supports Its Role in Controlling Auxin Traffic in LRs

The localization of the NRT1.1 protein strongly suggests that it participates in the basipetal reflux of auxin removing the hormone from the LR tip. Indeed, NRT1.1-GFP localization overlaps that of auxin carriers involved in this basipetal transport, such as PIN2 (Benkova et al., 2003), but is totally complementary to that of auxin carriers responsible for acropetal auxin transport (e.g., PIN1 and ABCB19/PGP19), which are expressed in the inner cell types of LRs (Benkova et al., 2003; Wu et al., 2007). Accordingly, *PIN2* mutation leads to increased auxin accumulation in LR primordia (Benkova et al., 2003), as it is the case for *NRT1.1* mutation (Figure 1), whereas mutations of either *PIN1* or *ABCB19/PGP19* result in the opposite effect (Benkova et al., 2003; Wu et al., 2007). Furthermore, the lack of any NRT1.1-GFP signal in LR primordia at early developmental stages (Figure 4G) agrees with the observation that neither NO_3^- nor loss of the NRT1.1 function altered *DR5::GUS* expression in the young primordia (Figure 1). This apparent absence of NRT1.1 in newly initiated primordia is an intriguing observation because the results obtained with *pNRT1.1::GUS* plants indicate a high level of *NRT1.1* transcription in the LR primordia at the earliest stages of development (Figure 4A; Guo et al., 2001). Interestingly, *NRT1.1* is not found in the list of genes displaying an increased mRNA level in response to massive initiation of LR primordia (Swarup et al., 2008; Vanneste et al., 2005). This shows that although *pNRT1.1* is activated during initiation of LR primordia (Guo et al., 2001), this may not result in a significant *NRT1.1* mRNA accumulation in these primordia, suggesting the occurrence of posttranscriptional control.

The apparent preferential localization of NRT1.1-GFP in anticlinal membranes may be illustrative of a polarized expression of NRT1.1 in LR epidermal cells (Figure 4; Figure S4). However, one must remain very cautious about this hypothesis. First, unlike the periclinal one, an anticlinal NRT1.1-GFP signal may arise from membranes of two adjacent cells, thus providing a simple explanation of its apparent higher intensity. Second, although the NRT1.1-GFP fusion protein is obviously functional (see Figure 4F), there is no guarantee that its precise localization is strictly identical to that of the native NRT1.1 protein. More thorough quantitative investigations at a higher resolution and including immunolocalization of the native protein are required. Nevertheless, subcellular polarization of NRT1.1 is not mandatory for its role in promoting basipetal transport of auxin.

A Model for Coupling NO_3^- Sensing by NRT1.1 and Lateral Root Development

As compared to high NO_3^- provision (1 mM or higher), growth of plants on an N-free medium results in a markedly decreased LR generation in the wild-type (Figure 2). This is due to two separate but additive effects: (1) a specific effect of the lack of NO_3^- that cannot be suppressed by provision of an alternative N source such as glutamine and is fully dependent on the repressive action of NRT1.1, and (2) a general effect of N starvation independent of NRT1.1 that reduces overall growth of both wild-type and *chl1* plants (Figure 2B) and that can be suppressed by glutamine (Figure 2). This latter effect explains why in the absence of NO_3^-, *NRT1.1* mutation is not sufficient to restore normal LR development as in wild-type plants grown on high
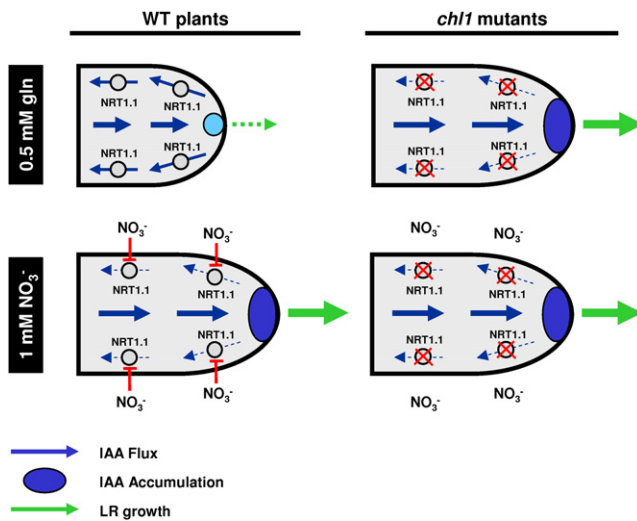
Figure 5. Schematic Model for NRT1.1 Control of Lateral Root Growth in Response to Nitrate

Two situations are shown to illustrate the specific effect of NO_3^- on lateral root growth, corresponding to plants supplied either with 0.5 mM glutamine or with 1 mM NO_3^- (1 mM external N in both cases). The model postulates that in the absence of NO_3^- (glutamine-fed plants), NRT1.1 favors basipetal transport of auxin in lateral roots, thus preventing auxin accumulation at the lateral root tip. This slows down outgrowth and elongation of lateral roots. At 1 mM NO_3^-, facilitation of basipetal auxin transport by NRT1.1 is inhibited, leading to auxin accumulation in the lateral root tip and accelerated growth of lateral root. Accordingly, *NRT1.1* mutation in *chl1* plants, which suppresses facilitation of basipetal auxin transport by NRT1.1, results in high auxin levels in the lateral root tip and accelerated growth of lateral roots, regardless of the external N source. Direct basipetal auxin transport by NRT1.1 is shown for simplicity to illustrate its facilitation of this transport flow.

NO_3^-, and why LR density in *chl1* mutants is reduced by N starvation (Figure 2).

Here we propose a model accounting for the specific effect of NO_3^- on LR growth (Figure 5). In wild-type plants grown in the absence or at low concentration of NO_3^- (glutamine-fed plants are depicted in Figure 5 to illustrate the specific NO_3^- effect), NRT1.1 facilitates auxin uptake into LR epidermal cells, thus promoting basipetal auxin transport and lowering auxin accumulation in the LR tip. This in turn represses LR growth. High NO_3^- concentration (~1 mM or higher) inhibits auxin transport facilitation by NRT1.1, allowing auxin to accumulate in LR tips, which stimulates LR growth. Accordingly, knockout mutation of *NRT1.1*, which suppresses NRT1.1 auxin transport facilitation in any situation, stimulates both auxin accumulation in LR tips and LR growth only in plants supplied with no NO_3^- (e.g., on glutamine medium) or with a low NO_3^- concentration, but not in plants grown on 1 mM NO_3^- or higher (Figure 5).

This model provides a working hypothesis for a mechanism of signal transduction by a mineral nutrient sensor/transceptor. We propose that the NO_3^--sensing function of NRT1.1 that controls lateral root growth is due to its dual NO_3^-/auxin transport activity, and that the NO_3^- signal transduced by NRT1.1 is an NO_3^--dependent modification of auxin transport in root tissues. A close link has been established in both plants and animals between nutrient and hormone signaling (Colombani et al., 2003; Moore et al., 2003; Nacry et al., 2005; Nero et al., 2009;

Rubio et al., 2009). However, we are not aware of any report suggesting that a molecular basis of this link can be related to the action of a nutrient/hormone dual substrate transporter/facilitator. As such, our model defines an original mechanism for nutrient sensing in higher organisms. It will be interesting to determine in the future whether this mechanism may explain the various NO_3^--signaling effects reported for NRT1.1, that is, stimulation of germination (Alboresi et al., 2005), regulation of the NO_3^- transporter gene *NRT2.1* (Ho et al., 2009; Krouk et al., 2006; Muños et al., 2004; Wang et al., 2009), and regulation of root growth and development (Remans et al., 2006; Walch-Liu and Forde, 2008). There are already some hints that this may not be the case. For instance, we found that the phenotype of the *chl1-5* mutant concerning LR growth is most pronounced in the absence of NO_3^- (Figure 2), whereas its phenotype concerning induction of *NRT2.1* is strongest at high NO_3^- concentration (Ho et al., 2009), suggesting the occurrence of separate signaling pathways for NRT1.1-dependent control of root growth and *NRT2.1* expression. The availability of several NRT1.1 mutants (e.g., T101A, T101D, P492L) differentially affected in transport/signaling functions (Ho et al., 2009; Walch-Liu and Forde, 2008) will certainly help determine whether this protein governs different responses of plants to NO_3^- through different sensing mechanisms.

EXPERIMENTAL PROCEDURES

Plant Stocks and Growth Conditions

chl1-5 (Tsay et al., 1993) and *chl1-10* (Muños et al., 2004) are in the Columbia (Col) and Wassilewskija (Ws) backgrounds, respectively. Both mutants lack NRT1.1 transcript (Muños et al., 2004; data not shown). *atnrt1.2-1* (Krouk et al., 2006) is in the Ws background. *DR5::GUS* transgenic plants (Ulmasov et al., 1997) (Col background) were crossed with *chl1-5* plants. Homozygous plants for both *chl1-5* mutation and *DR5::GUS* were screened on F2 (by PCR for *chl1-5* deletion) and F3 (*DR5::GUS* expression) offsprings. Surface sterilized seeds were sown in 12 × 12 cm transparent plates on 40 ml of solid medium (1% type A agar) containing 0.5 mM $CaSO_4$, 0.5 mM $MgCl_2$, 1 mM KH_2PO_4, 2.5 mM MES (2-[morpholino]ethanesulfonic acid) (pH 5.8), 50 μM NaFeEDTA, 50 μM H_3BO_3, 12 μM $MnCl_2$, 1 μM $CuCl_2$, 1 μM $ZnCl_2$, and 0.03 μM NH_4MoO_4. This basal medium was supplemented with KNO_3 and L-glutamine as nitrogen sources at the concentrations indicated in the figures (all chemicals are from Sigma). L-glutamine can sustain efficient growth of *Arabidopsis* plants and was used as an alternative N source to investigate the specific effect of NO_3^-. After storage for 2 days at 4°C in the dark, plates were incubated vertically in a growth chamber at 22°C with a 16 hr/8 hr light/dark regime and a light intensity of 230 $\mu mol.m^{-2}.s^{-1}$.

Production of the *pNRT1.1::NRT1.1-GFP* Transgenic Lines

Cloning of *pNRT1.1::NRT1.1* (5.688 kb fragment, including the 1.533 kbp 5′ untranslated region and promoting sequence upstream of the ATG and the genomic sequence of NRT1.1 without the stop codon) was amplified by PCR (NRT1.1 forward: tttgttctcgctcttccaca; NRT1.1 reverse: atgacccattggaa tactcg) and cloned in pENTR/D/TOPO entry vector, according to the manufacturer's instructions (Invitrogen). *pNRT1.1::NRT1.1-GFP* reporter construct was generated by making translational fusions of the cloned 5.688 kb NRT1.1 fragment and pGWB4 binary vector (no promoter, C-sGFP) obtained from Tsuyoshi Nakagawa (Research Institute of Molecular Genetics, Shimane University, Matsue, Japan) by LR recombination according to the manufacturer's recommendations (Invitrogen). Prior to transformation of *Agrobacterium*, the expression construct was sequenced. A binary vector containing the GFP fusion construct was introduced into *Agrobacterium tumefaciens* strain GC3101. *A. thaliana chl1-5* and *chl1-10* mutant plants were transformed by dipping the flowers in the presence of Silwet L77 (Clough and Bent, 1998). Transgenic seedlings were selected on a medium containing 30 mg/L of

hygromycin. For further analyses, T1 segregation ratios were analyzed to select transformants with one T-DNA insertion and to isolate T3-homozygous plants. Functionality of the construct was tested by restoring chlorate sensitivity (data not shown) and wild-type lateral root growth of transgenic seedlings.

Analysis of Root Growth

Vertical agar plates containing plants were scanned at 300 dpi (Epson Perfection 2450Photo; Seiko Epson), and root growth parameters were analyzed using Optimas image analysis software (MediaCybernetics), as described previously (Nacry et al., 2005). Analysis of the distribution of primordia and lateral roots between the various developmental stages was performed on 8-day-old seedlings according to the protocol described previously (Malamy and Benfey, 1997).

GUS Expression Analysis

Plantlets were vacuum infiltrated for 5 min and then incubated overnight at 37°C in reaction buffer containing 50 mM sodium phosphate buffer (pH 7), 0.5 mM ferricyanide, 0.5 mM ferrocyanide, 0.05% Triton X-100, and 1 mM X-Gluc. Plant pigments were cleared and GUS staining patterns were analyzed by an Olympus BX61 microscope and a digital camera (Colorview 2) driven by Analysis software (Soft Imaging System).

Confocal Microscopy

GFP images on lateral root primordia and lateral roots were acquired with a Zeiss LSM 510 META Axiovert 200M inverted microscope with objective C-Apochromat 40×/1.2 water immersion (Zeiss). GFP was excited with the 488 nm line of an argon laser and detected via a 505–530 nm band-pass filter (green). Propidium iodide (1 μg/ml) was used to stain cell walls and was excited with a 543 nm line argon laser and detected via a 585 nm long-pass filter (red). GFP imaging in yeast was performed using a Zeiss LSM 5 DUO confocal microscope (excitation 488 nm, emission 505–550 nm) with objective C-Apochromat 40× (NA = 1.2 W).

Oocyte Uptake Analysis

Oocytes obtained from *Xenopus laevis* (CRBM, CNRS, Montpellier, France) were defolliculated by a 1 hr collagenase treatment (1 mg/ml; type IA; Sigma) in a medium containing 82.5 mM NaCl, 2 mM KCl, 1 mM MgCl$_2$, and 5 mM HEPES-NaOH (pH 7.4). Stage V and VI oocytes were selected and placed at 18°C in a medium containing 96 mM NaCl, 2 mM KCl, 1.8 mM MgCl$_2$, 1 mM CaCl$_2$, 2.5 mM Na-pyruvate, and 5 mM HEPES-NaOH (pH 7.4) supplemented with 50 mg/ml gentamicin. Oocytes were injected (50 nl) with cRNA (NRT1.1, NRT1.2, AUX1, or LAX3; 500 ng/μl) using a 10–15 μm tip diameter micropipette and a pneumatic injector. Control oocytes were either not injected or injected with 50 nl of water. $^{15}NO_3^-$ and [^{3}H]IAA uptake analyses were adapted from Tsay et al. (1993) and Yang et al. (2006), respectively. Briefly, for $^{15}NO_3^-$ uptake, batches of 30 oocytes (injected or control ones) were incubated for 3 hr in 2 ml of Ringer medium (pH 5.5) containing 30 mM K^{15}NO$_3$ (atom % ^{15}N abundance: 99.9%; Courtage Analyses Services). Oocytes were then washed five times in 50 ml of NO$_3^-$ free Ringer medium at 4°C. Batches of five oocytes were then analyzed for total N content and atom % ^{15}N abundance by continuous-flow mass spectrometry using an Euro-EA Eurovector elemental analyzer coupled with an IsoPrime mass spectrometer (GV Instruments). For IAA uptake, oocytes were incubated for 20 min in 1 ml of Ringer solution (pH 6; according to Yang et al., 2006) containing 1 μM [^{3}H]IAA (100 nM [^{3}H]IAA; GE Healthcare; diluted with 900 nM cold-IAA; Sigma). They were then washed five times in 50 ml of Ringer solution (4°C) containing 5 μM cold-IAA. Each oocyte was then dissolved in 50 μl of 2% SDS. Lysis solution was then mixed with 3 ml of scintillating solution. Incorporated radioactivity was measured by liquid scintillation analyzer (Tri-Carb 2100TR; Packard Instrument).

IAA Uptake in Seedlings

Seedlings were grown for 4 days on solid basal medium without nitrogen or supplemented with 1 mM L-glutamine or 10 mM KNO$_3$. Five batches of ten seedlings each were preincubated for 20 min in 12 ml of liquid basal medium (pH 5.8) and transferred for 30 min to 3 ml of liquid basal medium containing 1 μM [^{3}H]IAA. They were then washed five times in 12 ml of liquid basal medium

(4°C) containing 5 μM cold-IAA. Incorporated radioactivity was measured on the five replicate batches by liquid scintillation analyzer (Tri-Carb 2100TR; Packard Instrument).

IAA Uptake in Yeast

cDNA of NRT1.1 was subcloned into pVT100-U and pVT100-U-GFP yeast expression vectors. Resulting plasmids were transformed into *S. cerevisiae* BY4742 strain (Euroscarf) generating strains NRT1.1 and NRT1.1-GFP used in this study. Strain BY4742 transformed with empty vector pVT100-U was used as a control. The exponentially growing yeast cells were harvested by centrifugation and resuspended in MES buffer (pH 4.6) with 2% glucose. ^{3}H-labeled IAA (American Radiolabeled Chemicals; specific radioactivity 20 Ci/mmol) was added to the cells and aliquots were taken at indicated time points. Cells were collected on membrane filters and washed extensively. The filters were placed in scintillation liquid and radioactivity was measured using liquid scintillation counting (Tri-Carb 2900TR; Packard Instrument).

IAA Analysis

Root tissue was pooled, weighed, and frozen in liquid nitrogen for quantification of free IAA content. [$^{13}C_6$]IAA internal standard (Cambridge Isotope Laboratories) was added to each sample at a concentration of 50 pg/mg fresh weight, and the samples were then homogenized, extracted, and purified as described previously (Andersen et al., 2008). After derivatization, the samples were analyzed by gas chromatography–selected reaction monitoring mass spectrometry as described previously (Edlund et al., 1995).

IAA and NRT1.1 Immunolocalization

Eight-day-old seedlings were prefixed in 3% EDAC/PBS for 1 hr at room temperature (this step was included only for purposes of IAA detection) and fixed in 4% paraformaldehyde in PBS/0.1% Triton X-100. Seedlings were washed twice for 10 min in PBS and twice for 10 min in water, mounted on SuperFrost slides, and dried. A rehydration step (10 min in PBS) was followed by incubation in 1.5% Driselase/PBS for 40 min at 37°C. After four washes with PBS, seedlings were permeabilized by incubation in 1% NP-40/10% DMSO in PBS for 1 hr, washed six times with PBS, and incubated in blocking buffer (3% BSA/PBS) for 2 hr at 37°C. Permeabilized seedlings were incubated with primary monoclonal anti-auxin mouse antibody (Sigma) (dilution 1:100) or anti-GFP antibodies (Roche), diluted 1:1000 in blocking buffer for 5 hr in a humid chamber at 37°C, washed five times for 5 min in PBS, and further incubated overnight at 4°C with a secondary antibody (anti-mouse IgG AP conjugate; Sigma) or Alexa Fluor 488 (Invitrogen) goat anti-mouse diluted 1:800. After several rinses, the secondary antibody was detected either with western blue-stabilized substrate for alkaline phosphatase (Promega) or using confocal laser-scanning microscopy, with a Leica TCS SP2 AOBS, respectively.

Western Blot Analysis

Microsomes were prepared as described previously (Giannini et al., 1987) from seedlings grown for 12 days in liquid medium. Proteins were separated on denaturing SDS-PAGE followed by an electrotransfer at 4°C onto a nitrocellulose membrane (Sartorius). NRT1.1-GFP was detected using a anti-GFP-HRP antibody (Miltenyi Biotech). The immunodetection was performed with a chemiluminescent detection system kit (SuperSignal; Pierce).

Statistical Analyses

Data are presented as means ± SEM, and have been analyzed using ANOVA and/or Student's t test.

SUPPLEMENTAL INFORMATION

Supplemental Information includes four figures and can be found with this article online at doi:10.1016/j.devcel.2010.05.008.

REFERENCES

Alboresi, A., Gestin, C., Leydecker, M.T., Bedu, M., Meyer, C., and Truong, H.N. (2005). Nitrate, a signal relieving seed dormancy in *Arabidopsis*. Plant Cell Environ. *28*, 500–512.

Andersen, S.U., Buechel, S., Zhao, Z., Ljung, K., Novak, O., Busch, W., Schuster, C., and Lohmann, J.U. (2008). Requirement of B2-type cyclin-dependent kinases for meristem integrity in *Arabidopsis thaliana*. Plant Cell *20*, 88–100.

Benjamins, R., and Scheres, B. (2008). Auxin: the looping star in plant development. Annu. Rev. Plant Biol. *59*, 443–465.

Benkova, E., Michniewicz, M., Sauer, M., Teichmann, T., Seifertova, D., Jurgens, G., and Friml, J. (2003). Local, efflux-dependent auxin gradients as a common module for plant organ formation. Cell *115*, 591–602.

Blakeslee, J.J., Bandyopadhyay, A., Lee, O.R., Mravec, J., Titapiwatanakun, B., Sauer, M., Makam, S.N., Cheng, Y., Bouchard, R., Adamec, J., et al. (2007). Interactions among PIN-FORMED and P-glycoprotein auxin transporters in *Arabidopsis*. Plant Cell *19*, 131–147.

Blilou, I., Xu, J., Wildwater, M., Willemsen, V., Paponov, I., Friml, J., Heidstra, R., Aida, M., Palme, K., and Scheres, B. (2005). The PIN auxin efflux facilitator network controls growth and patterning in *Arabidopsis* roots. Nature *433*, 39–44.

Casimiro, I., Beeckman, T., Graham, N., Bhalerao, R., Zhang, H., Casero, P., Sandberg, G., and Bennett, M.J. (2003). Dissecting *Arabidopsis* lateral root development. Trends Plant Sci. *8*, 165–171.

Clough, S.J., and Bent, A.F. (1998). Floral dip: a simplified method for *Agrobacterium*-mediated transformation of *Arabidopsis thaliana*. Plant J. *16*, 735–743.

Colombani, J., Raisin, S., Pantalacci, S., Radimerski, T., Montagne, J., and Leopold, P. (2003). A nutrient sensor mechanism controls *Drosophila* growth. Cell *114*, 739–749.

Crawford, N.M. (1995). Nitrate: nutrient and signal for plant growth. Plant Cell *7*, 859–868.

De Smet, I., Tetsumura, T., De Rybel, B., Frey, N.F., Laplaze, L., Casimiro, I., Swarup, R., Naudts, M., Vanneste, S., Audenaert, D., et al. (2007). Auxin-dependent regulation of lateral root positioning in the basal meristem of *Arabidopsis*. Development *134*, 681–690.

Edlund, A., Eklof, S., Sundberg, B., Moritz, T., and Sandberg, G. (1995). A microscale technique for gas chromatography-mass spectrometry measurements of picogram amounts of indole-3-acetic acid in plant tissues. Plant Physiol. *108*, 1043–1047.

Forde, B.G. (2002). Local and long-range signaling pathways regulating plant responses to nitrate. Annu. Rev. Plant Biol. *53*, 203–224.

Giannini, J.L., Gildensoph, L.H., Reynolds-Niesman, I., and Briskin, D.P. (1987). Calcium transport in sealed vesicles from red beet (*Beta vulgaris* L.) storage tissue: I. Characterization of a Ca-pumping ATPase associated with the endoplasmic reticulum. Plant Physiol. *85*, 1129–1136.

Gojon, A., Nacry, P., and Davidian, J.C. (2009). Root uptake regulation: a central process for NPS homeostasis in plants. Curr. Opin. Plant Biol. *12*, 328–338.

Guo, F.Q., Wang, R., Chen, M., and Crawford, N.M. (2001). The *Arabidopsis* dual-affinity nitrate transporter gene *AtNRT1.1 (CHL1)* is activated and functions in nascent organ development during vegetative and reproductive growth. Plant Cell *13*, 1761–1777.

Guo, F.-Q., Wang, R., and Crawford, N.M. (2002). The *Arabidopsis* dual-affinity nitrate transporter gene *AtNRT1.1 (CHL1)* is regulated by auxin in both shoots and roots. J. Exp. Bot. *53*, 835–844.

Ho, C.H., Lin, S.H., Hu, H.C., and Tsay, Y.F. (2009). CHL1 functions as a nitrate sensor in plants. Cell *138*, 1184–1194.

Hoch, J.A. (2000). Two-component and phosphorelay signal transduction. Curr. Opin. Microbiol. *3*, 165–170.

Holsbeeks, I., Lagatie, O., Van Nuland, A., Van de Velde, S., and Thevelein, J.M. (2004). The eukaryotic plasma membrane as a nutrient-sensing device. Trends Biochem. Sci. *29*, 556–564.

Huang, N.C., Liu, K.H., Lo, H.J., and Tsay, Y.F. (1999). Cloning and functional characterization of an *Arabidopsis* nitrate transporter gene that encodes a constitutive component of low-affinity uptake. Plant Cell *11*, 1381–1392.

Kramer, E.M., and Bennett, M.J. (2006). Auxin transport: a field in flux. Trends Plant Sci. *11*, 382–386.

Krouk, G., Tillard, P., and Gojon, A. (2006). Regulation of the high-affinity NO_3^- uptake system by NRT1.1-mediated NO_3^- demand signaling in *Arabidopsis*. Plant Physiol. *142*, 1075–1086.

Krouk, G., Crawford, N.M., Coruzzi, G.M., and Tsay, Y.F. (2010). Nitrate signaling: adaptation to fluctuating environments. Curr. Opin. Plant Biol.. in press.

Laskowski, M., Grieneisen, V.A., Hofhuis, H., Hove, C.A., Hogeweg, P., Maree, A.F., and Scheres, B. (2008). Root system architecture from coupling cell shape to auxin transport. PLoS Biol. *6*, e307.

Liu, K.H., and Tsay, Y.F. (2003). Switching between the two action modes of the dual-affinity nitrate transporter CHL1 by phosphorylation. EMBO J. *22*, 1005–1013.

Malamy, J.E. (2005). Intrinsic and environmental response pathways that regulate root system architecture. Plant Cell Environ. *28*, 67–77.

Malamy, J.E., and Benfey, P.N. (1997). Organization and cell differentiation in lateral roots of *Arabidopsis thaliana*. Development *124*, 33–44.

Moore, B., Zhou, L., Rolland, F., Hall, Q., Cheng, W.H., Liu, Y.X., Hwang, I., Jones, T., and Sheen, J. (2003). Role of the *Arabidopsis* glucose sensor HXK1 in nutrient, light, and hormonal signaling. Science *300*, 332–336.

Muños, S., Cazettes, C., Fizames, C., Gaymard, F., Tillard, P., Lepetit, M., Lejay, L., and Gojon, A. (2004). Transcript profiling in the *chl1-5* mutant of *Arabidopsis* reveals a role of the nitrate transporter NRT1.1 in the regulation of another nitrate transporter, NRT2.1. Plant Cell *16*, 2433–2447.

Nacry, P., Canivenc, G., Muller, B., Azmi, A., Van Onckelen, H., Rossignol, M., and Doumas, P. (2005). A role for auxin redistribution in the responses of the root system architecture to phosphate starvation in *Arabidopsis*. Plant Physiol. *138*, 2061–2074.

Nero, D., Krouk, G., Tranchina, D., and Coruzzi, G.M. (2009). A system biology approach highlights a hormonal enhancer effect on regulation of genes in a nitrate responsive "biomodule." BMC Syst. Biol. *3*, 59.

Petrasek, J., Mravec, J., Bouchard, R., Blakeslee, J.J., Abas, M., Seifertova, D., Wisniewska, J., Tadele, Z., Kubes, M., Covanova, M., et al. (2006). PIN proteins perform a rate-limiting function in cellular auxin efflux. Science *312*, 914–918.

Remans, T., Nacry, P., Pervent, M., Filleur, S., Diatloff, E., Mounier, E., Tillard, P., Forde, B.G., and Gojon, A. (2006). The *Arabidopsis* NRT1.1 transporter participates in the signaling pathway triggering root colonization of nitrate-rich patches. Proc. Natl. Acad. Sci. USA *103*, 19206–19211.

Rubio, V., Bustos, R., Irigoyen, M.L., Cardona-Lopez, X., Rojas-Triana, M., and Paz-Ares, J. (2009). Plant hormones and nutrient signaling. Plant Mol. Biol. *69*, 361–373.

Schachtman, D.P., and Shin, R. (2007). Nutrient sensing and signaling: NPKS. Annu. Rev. Plant Biol. *58*, 47–69.

Stitt, M. (1999). Nitrate regulation of metabolism and growth. Curr. Opin. Plant Biol. *2*, 178–186.

Swarup, K., Benkova, E., Swarup, R., Casimiro, I., Peret, B., Yang, Y., Parry, G., Nielsen, E., De Smet, I., Vanneste, S., et al. (2008). The auxin influx carrier LAX3 promotes lateral root emergence. Nat. Cell Biol. *10*, 946–954.

Teale, W.D., Paponov, I.A., and Palme, K. (2006). Auxin in action: signalling, transport and the control of plant growth and development. Nat. Rev. Mol. Cell Biol. *7*, 847–859.

Tsay, Y.F., Schroeder, J.I., Feldmann, K.A., and Crawford, N.M. (1993). The herbicide sensitivity gene *CHL1* of *Arabidopsis* encodes a nitrate-inducible nitrate transporter. Cell *72*, 705–713.

Ulmasov, T., Murfett, J., Hagen, G., and Guilfoyle, T.J. (1997). Aux/IAA proteins repress expression of reporter genes containing natural and highly active synthetic auxin response elements. Plant Cell *9*, 1963–1971.

Vanneste, S., and Friml, J. (2009). Auxin: a trigger for change in plant development. Cell *136*, 1005–1016.

Vanneste, S., De Rybel, B., Beemster, G.T., Ljung, K., De Smet, I., Van Isterdael, G., Naudts, M., Iida, R., Gruissem, W., Tasaka, M., et al. (2005). Cell cycle progression in the pericycle is not sufficient for SOLITARY ROOT/IAA14-mediated lateral root initiation in *Arabidopsis thaliana*. Plant Cell *17*, 3035–3050.

Vieten, A., Sauer, M., Brewer, P.B., and Friml, J. (2007). Molecular and cellular aspects of auxin-transport-mediated development. Trends Plant Sci. *12*, 160–168.

Walch-Liu, P., and Forde, B.G. (2008). Nitrate signalling mediated by the NRT1.1 nitrate transporter antagonises L-glutamate-induced changes in root architecture. Plant J. *54*, 820–828.

Wang, R., Xing, X., Wang, Y., Tran, A., and Crawford, N.M. (2009). A genetic screen for nitrate regulatory mutants captures the nitrate transporter gene NRT1.1. Plant Physiol. *151*, 472–478.

Williams, L., and Miller, A.J. (2001). Transporters responsible for the uptake and partitioning of nitrogenous solutes. Annu. Rev. Plant Physiol. Plant Mol. Biol. *52*, 659–688.

Wipf, D., Ludewig, U., Tegeder, M., Rentsch, D., Koch, W., and Frommer, W.B. (2002). Conservation of amino acid transporters in fungi, plants and animals. Trends Biochem. Sci. *27*, 139–147.

Wu, G., Lewis, D.R., and Spalding, E.P. (2007). Mutations in *Arabidopsis* multidrug resistance-like ABC transporters separate the roles of acropetal and basipetal auxin transport in lateral root development. Plant Cell *19*, 1826–1837.

Yang, H., and Murphy, A.S. (2009). Functional expression and characterization of *Arabidopsis* ABCB, AUX1 and PIN auxin transporters in *Schizosaccharomyces pombe*. Plant J. *59*, 179–191.

Yang, Y., Hammes, U.Z., Taylor, C.G., Schachtman, D.P., and Nielsen, E. (2006). High-affinity auxin transport by the AUX1 influx carrier protein. Curr. Biol. *16*, 1123–1127.

Zhang, H., Jennings, A., Barlow, P.W., and Forde, B.G. (1999). Dual pathways for regulation of root branching by nitrate. Proc. Natl. Acad. Sci. USA *96*, 6529–6534.

Zhou, J.J., Theodoulou, F.L., Muldin, I., Ingermarsson, B., and Miller, A.J. (1998). Cloning and functional characterization of a *Brassica napus* transporter that is able to transport nitrate and histidine. J. Biol. Chem. *273*, 12017–12023.